VIABILITY OF A BIOLOGICAL PEST CONTROL AGENT THROUGH HYDRAULIC NOZZLES

J. P. Fife, H. E. Ozkan, R. C. Derksen, P. S. Grewal, C. R. Krause

ABSTRACT. *Exposure to hydrodynamic stresses during flow through a hydraulic nozzle can cause permanent damage to biological pesticides during spray application. Aqueous suspensions of a benchmark biological pest control agent, entomopathogenic nematodes (EPNs), were passed through three different hydraulic nozzles (standard flat fan, Spraying Systems XR8001VS; hollow cone, Spraying Systems TXA8001VK; and full cone, Spraying Systems FL5−VS) within an experimental, opposed−pistons flow device. Computational fluid dynamics (CFD) was used to numerically simulate the internal flow within the XR8001VS and TXA8001VK nozzles, and important flow field parameters from the CFD simulations were compared to the observed EPN relative viability after treatment. Overall, greater reductions in EPN relative viability were observed for the flat fan (9.5%) compared to the cone type nozzles (≤2.8%). The average energy dissipation rates within the exit orifices were significantly higher for the XR8001VS flat fan compared to the TXA8001VK hollow cone, which was consistent with the greater reductions in EPN relative viability observed for the XR8001VS. These differences in EPN damage were due to the distinct characteristics of each nozzle's flow field. The reduced flow area of the narrow, elliptical exit orifice of the flat fan generates an extensional flow regime, where it was found that the tensile stresses developed were large enough to cause nematode damage. However, with the cone nozzles, the high rotational flow component did not produce hydrodynamic conditions conducive to causing nematode damage. Overall, common hydraulic nozzles were found to be acceptable for spray application of EPNs following the manufacturer's recommendations. However, it is recommended that an appropriately sized (i.e., larger than the organism) cone nozzle is more suitable for spray application than a fan nozzle to avoid damage to the biopesticide.*

Keywords. *Biopesticides, CFD, Energy dissipation rate, Entomopathogenic nematodes, Hydraulic nozzles, Hydrodynamic stresses.*

Modern crop protection seeks to manage pests rather than completely control them. Thus, the trend in agricultural and horticultural practices is a conversion from traditional, broad−spectrum chemical pesticides to highly specific chemical and biologically based products to be used as part of an integrated pest management (IPM) program (Caulder, 1999). Nonetheless, concern over issues related to the non−target activity of chemical pesticides remains, and biological pesticides (i.e., biopesticides) are receiving increased attention as safer, more environmentally friendly alternatives to chemical pesticides and as key components of IPM (Copping and Menn, 2000).

Yet, few biopesticides are currently being used commercially as alternatives to chemical pesticides (Gan−Mor and Matthews, 2003) and represent little more than 1% of the total world pesticide market (Menn and Hall, 1999). Biopesticides are mainly being used in niche markets where no effective chemical pesticides are available, on organic farms, and where high−value crops are being grown under controlled conditions (Jacobsen and Backman, 1993). Grower acceptance of biopesticides has been limited primarily by the relative cost compared to chemical pesticides, limited shelf life, difficulties in handling and delivery, and variable field performance (Copping and Menn, 2000).

Research and development efforts have mainly involved the production and formulation technologies of biopesticides, while the methods for delivery have not been adequately considered (Gan−Mor and Matthews, 2003). In contrast to chemical pesticides, biopesticides are living systems (e.g., bacteria, fungi, viruses, predators, and parasites), which introduce additional challenges with respect to formulation and delivery because, in order to be effective, the biological agents must remain viable during the application process. At present, there are few research−based guidelines on how biopesticides should be applied to optimize their performance in the field. Such guidelines are critical for increased acceptance and use of biopesticides by growers.

Debate continues as to whether existing, conventional spray equipment is acceptable, or if new equipment and

Article was submitted for review in December 2003; approved for publication by the Power & Machinery Division of ASAE in November 2004. Presented at the 2003 ASAE Annual Meeting as Paper No. 031063.

Names are necessary to report factually on available data; however, the USDA and The Ohio State University neither guarantee nor warrant the standard of the product, and the use of the name by USDA or OSU implies no approval of the product to the exclusion of others that may also be suitable.

The authors are **Jane Patterson Fife, ASAE Member Engineer,** Research Scientist, Battelle Memorial Institute, Columbus, Ohio; **H. Erdal Ozkan, ASAE Member Engineer,** Professor, FABE, The Ohio State University, Columbus, Ohio; **Richard C.Derksen, ASAE Member Engineer,** Agricultural Engineer, and **Charles R. Krause,** Research Leader, USDA−ARS Application Technology Research Unit, OARDC, Wooster, Ohio; and **Parwinder S. Grewal,** Associate Professor, Department of Entomology, The Ohio State University, OARDC, Wooster, Ohio. **Corresponding author:** Jane Patterson Fife, 505 King Ave., Columbus, OH 43201; phone: 614−424−3186; fax: 614−424−4185; e−mail: fifej@battelle.org.

delivery systems need to be developed for application of biological agents. Commercially, the implementation of biopesticides is most likely to come about with the development of products that can be applied using conventional equipment, as growers are unlikely to invest in new spray equipment or radically alter their practices (Bateman, 1999). Others argue that the success of biopesticides is dependent on the development of new delivery systems that can effectively handle, meter, and disperse the biopesticides so that the organisms are placed where they need to be, when they need to be there, and in a viable form (Gan−Mor and Matthews, 2003; Steinke and Giles, 1995). In practice, different kinds of sprayers, mostly hydraulic, are being used to apply some biopesticides, as there are currently no special delivery systems commercially available (Nilsson and Gripwall, 1999). However, before new delivery systems are considered for development, the limitations of existing equipment need to be investigated.

A common equipment component to most liquid application systems is a hydraulic nozzle (e.g., flat fan, cone), where liquid under pressure is forced through a small orifice to form droplets (Matthews, 1992). This equipment was based on technology developed for application of broad−spectrum chemical pesticides and may not be suitable for biological agents (Steinke and Giles, 1995). A variety of hydrodynamic stresses are developed during flow through a hydraulic nozzle that may cause damage to a biological agent. A better understanding of the hydrodynamic stresses developed within the nozzles is necessary to provide recommendations of the appropriate nozzle characteristics and operating conditions for effective application of biopesticides.

The overall goal of this study was to evaluate the effects of two common types of hydraulic nozzles (standard flat fan and cone) on damage to a benchmark biological pest control agent, entomopathogenic nematodes (EPNs). We hypothesize that the approximately elliptical exit orifice of a flat fan nozzle will introduce greater hydrodynamic stress, and consequently greater reductions in EPN viability, compared to the circular exit orifice of a cone nozzle. Therefore, the specific objectives of this study were: (1) to quantify the EPN relative viability after flow through each nozzle type within an experimental flow device, (2) to simulate the internal flow within each nozzle type using numerical methods, and (3) to compare experimental results with important flow field parameters from the numerical simulations of the nozzles.

Materials and Methods

Entomopathogenic Nematodes

Entomopathogenic nematodes were selected as the benchmark biological pest control agent because they are relatively robust, multicellular organisms. Four species of entomopathogenic nematodes (EPNs) were studied based on their family and relative size: *Heterorhabditis bacteriophora* (Poinar) GPS 11 strain, *H. megidis* (Poinar, Jackson and Klein) UK strain, *Steinernema carpocapsae* (Weiser) All strain, and *S. glaseri* (Steiner) NJ strain. The average lengths and widths of the infective juvenile *S. carpocapsae* are 558 × 25 μm, of *H. bacteriophora* 588 × 23 μm, of *H. megidis* 768 × 29 μm, and of *S. glaseri* 1130 × 43 μm (Poinar, 1990).

The nematodes were cultured *in vivo* in the laboratory using last−instar *Galleria mellonella* (L.) (Vanderhorst Canning Co., St. Mary's, Ohio) as the host and standard culture procedures (Kaya and Stock, 1997). The harvested nematodes, in the infective juvenile (IJ) stage, were placed in a 500 mL beaker. After 15 min, the liquid from the top, which contained dead nematodes and debris, was decanted. The concentrated suspension was then slowly poured over a tissue paper, wetted, and draped over a mesh screen on top of a 150 × 20 mm petri dish to separate the living nematodes from the dead nematodes. The filtered suspensions were diluted with tap water to concentrations between 1000 and 2000 EPNs mL^{-1}, and 60 mL aliquots were individually stored in 150 × 20 mm petri dishes at 10°C until tests were conducted. All tests were conducted within two weeks following harvest. For each test suspension, the relative viability of three 100 μL subsamples was evaluated prior to testing and served as a control. The overall relative viability of control suspensions was 99.2% (SE 0.2%).

Experimental Flow Device

The experiments were conducted using an opposed−pistons flow device developed by Clay and Koelling (1997). The experimental flow device provided a system to evaluate the hydrodynamic conditions developed during internal flow within the hydraulic nozzles, minimizing effects due to pumping or atomization. The source of energy for the fluid movement is the motion of the piston. The liquid exiting the nozzle orifice should remain in a liquid continuum as it fills the volume made available by the retracting piston. Therefore, the formation of droplets and the large pressure drop to atmosphere normally encountered in practice at the nozzle exit orifice should not occur with the flow device. Thus, it is reasonable to assume that any observed reduction in EPN relative viability resulted from the hydrodynamic conditions within the hydraulic nozzle.

As shown in figure 1, the device consists of two high−pressure pipes (stainless steel, 1.45 cm diameter, 35.56 cm length) (High Pressure Equipment, Erie, Pa.) that are coupled with an orifice plate (stainless steel, 1.45 cm orifice diameter, 0.18 cm plate thickness). A stainless steel gasket was specially made to hold the plastic casings of the nozzles within the orifice plate opening. Two pistons in the device (stainless steel, 1.44 cm diameter, 30.48 cm stroke length) (High Pressure Equipment) are moved in phase by a hydraulic system, so that as one piston moves forward, forcing the suspension through the pipe and nozzle, the other piston retracts on the collection side. The hydraulic system consists of a 3.73 kW, 1800 rpm, TEFC motor (Lincoln Electric Co., Cleveland, Ohio) and a variable volume, pressure−compensated control pump (The Oilgear Co., Milwaukee, Wisc.). The entire hydraulic system is mounted on a 57 L oil reservoir, and includes a dual flow control valve, a lever−operated directional valve, and a 50 μm return filter. The hydraulic pumping system drives the two hydraulic cylinders (J−series, Miller Fluid Power, Bensenville, Ill.).

Prior to each test, the piston speed was measured using a digital tachometer (DT−107, Shimpo, Japan), and any adjustments to the piston speed were made at this time. All tests were within 0.04 cm s^{-1} (SE = 0.001 cm s^{-1}) of the desired piston speed. The pressure within the flow device could not be measured due to the tolerance between the piston and the tube. Thus, the piston speed was the controlled variable for the experiments, from which the volumetric flow rate was estimated.

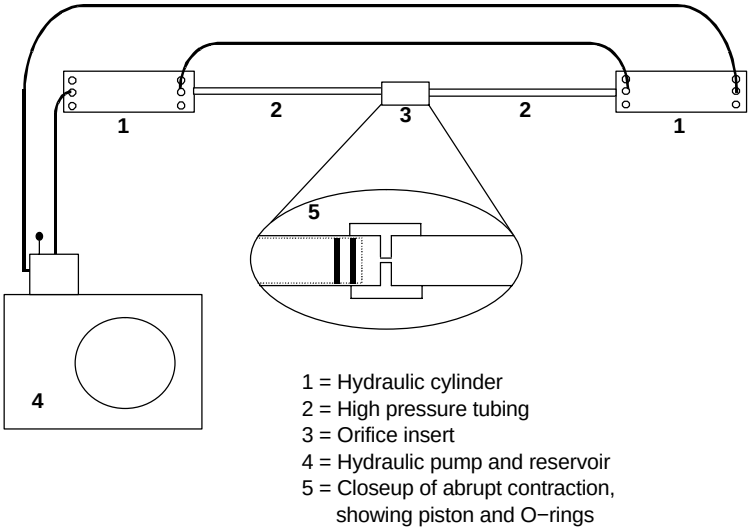

Figure 1. Schematic diagram of the opposed−pistons flow device developed by Clay and Koelling (1997) that was used in the experiments.

Three hydraulic nozzles were tested: standard flat fan (Spraying Systems XR8001VS, Spraying Systems Co., Wheaton, Ill.), hollow cone (Spraying Systems TXA8001VK), and full cone (Spraying Systems FL5−VS). The XR8001VS and FL5−VS nozzles were selected for this study because they are the smallest commercially available nozzles of their types and represent worst case scenarios with respect to possible hydrodynamic conditions. The TXA8001VK nozzle was selected because it is similar in capacity to the XR8001VS, but smaller capacity nozzles of this type are also commercially available. All nozzles were new prior to testing.

Immediately before conducting the individual tests, the EPN suspensions were thoroughly mixed and approximately 50 mL of the suspension was loaded into the pipe, between the piston and the nozzle. All EPNs were assumed to have passed through the nozzle orifice based on preliminary evaluations. The total time for loading, running the test, and unloading the sample was less than 10 min. Tests were conducted at piston speeds of 13, 17, and 21 cm s^{-1}, corresponding to volumetric flow rates of 1.3, 1.7, and 2.1 L min^{-1}, respectively. Tests at each flow rate were repeated two times for each nozzle. Treatment order was not randomized.

The manufacturer (Spraying Systems Co.) recommendations operating pressures (and corresponding volumetric flow rates) for the XR8001VS, TXA8001VK, and FL5−VS nozzles of 103 to 414 kPa (0.2 to 0.5 L min^{-1}), 276 to 862 kPa (0.4 to 0.6 L min^{-1}), and 103 to 276 kPa (1.3 to 2.0 L min^{-1}), respectively. The volumetric flow rates tested in this study were considerably higher than the recommendations for the XR8001VS and TXA8001VK nozzles and within the same range as for the FL5−VS nozzle.

Quantification of Nematode Relative Viability

Nematode relative viability was quantified following the procedure of Fife et al. (2003). Nematodes were counted by collecting a 100 µL subsample with a micro−dispenser from a thoroughly mixed suspension, and adding approximately 10 mL of water in a 55 × 10 mm petri dish to allow for easy viewing with the light microscope. Three subsamples per replication were counted for all treatments. Nematode relative viability was determined by separately recording the number of live (*L*), dead (*D*), half pieces (*HP*), and quarter pieces (*QP*) of nematodes. Nematodes were considered dead if they were broken or did not respond to prodding. The relative viability (*RV*, %) of the nematodes after treatment was computed as follows:

$$RV = \left(\frac{L}{L + D + \frac{HP}{2} + \frac{QP}{4}} \right) \times 100 \qquad (1)$$

Statistical Analyses

Data on relative viability of EPNs were arcsine transformed because the majority of data varied between 70% and 100%, and the transform spread out the data near 100% to increase their variance (Snedecor and Cochran, 1989). The arcsine transformed data were analyzed by a completely randomized, 4 × 3 × 3 factorial ANOVA with subsampling, and EPN species, nozzle type, and flow rate treatment effects, respectively. The treatment and total sums of squares were determined using the PROC GLM procedure in SAS (SAS, 1994). The subsampling sum of squares was determined by computing the sum of squares for each set of subsamples and then summing these values. The error sum of squares was computed from the residual. Least significant differences (LSD) were used to compare individual treatment means at a significance level of 0.05.

Computer Simulation of the Nozzle Flow Fields

The internal flow fields of the two similar capacity hydraulic nozzles (XR8001VS flat fan, TXA8001VK hollow cone) were simulated using FLUENT (Version 6.0, FLUENT, Inc., Lebanon, N.H.). A representative nozzle of each type was cut in half, and the internal dimensions were measured using a digital caliper (No. 500−115, Mitutoyo, Japan) and cold field emission scanning electron microscope (CFE−SEM) (Hitachi model S−4700, Nissei Sangyo Instruments, Inc., Mountain View, Cal.) micrographs of each nozzle's cross−section. The nozzle cross−sections were gold plated and placed on the specimen stub. The prepared stub was examined with the CFE−SEM at accelerating voltages ranging between 15 and 20 kV, working distances between

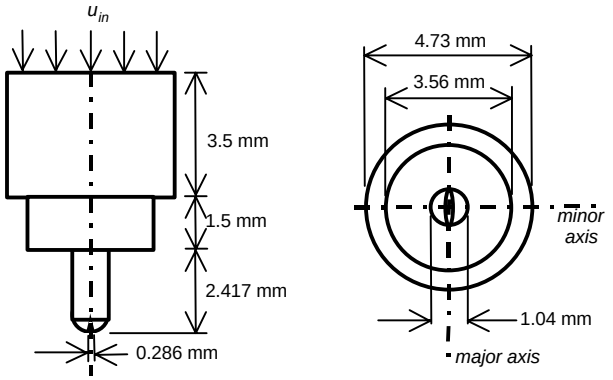

Figure 2. Schematic diagram of the Spraying Systems XR8001VS flat fan nozzle.

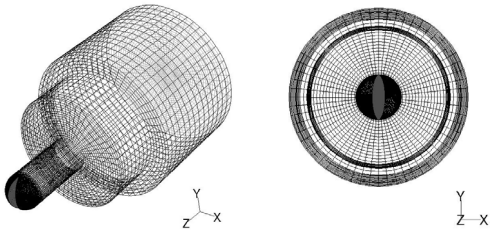

Figure 3. Grid mesh of the XR8001VS flat fan nozzle used in FLUENT to simulate the flow field.

4.4 and 9.9 mm, and magnifications between 30X and 40X. The three−dimensional geometry for each nozzle was created in GAMBIT (Version 2.0.4, FLUENT, Inc., Lebanon, N.H.), the preprocessor for FLUENT.

Flat Fan Nozzle

A diagram of the internal structure of an XR8001VS nozzle tip is presented in figure 2. The internal shape of a standard fan nozzle causes liquid from a single direction to curve inwards so the two streams of liquid meet at the elliptical exit orifice, producing the characteristic fan−patterned, thin sheet (Matthews, 1992).

A Cartesian coordinate system was used, with *z* in the axial direction. The geometry consists of three superimposed cylinders with the following radii (*R*, mm) and lengths (*L*, mm): R_1 = 2.365 mm, L_1 = 3.5 mm; R_2 = 1.78 mm, L_2 = 1.5 mm; and R_3 = 0.52 mm, L_3 = 2.0 mm. A sphere with a radius of 0.5279 mm was split by a plane located 0.091 mm from the center of the sphere. The smaller portion of the sphere was superimposed onto the end of the third cylinder. A wedge (0.417 mm height, 0.286 mm base) was removed from the sphere to create the approximately elliptical exit orifice. The dimensions of the major and minor axes of the elliptical orifice are 0.52 and 0.286 mm, respectively. The grid mesh used for the FLUENT simulations of the XR8001VS nozzle is presented in figure 3. The volume mesh is a hexahedral and tetrahedral hybrid. The grid volumes are non−uniform, with the concentration of volumes around the nozzle axis and outlet. There is a tradeoff between the resolution of the simulation results (i.e., total number of computational nodes) and the time to run the simulation, so several different mesh schemes were analyzed to determine an appropriate grid independent solution. A total of 159,080 nodes were used in the model, with 70% of those nodes located in the exit orifice region. The grid size within the exit orifice region is approximately 10 µm, which is over two times smaller than the average width of an EPN.

Hollow Cone Nozzle

A diagram of the internal structure of a TXA8001VK nozzle tip is presented in figure 4. The liquid is forced through tangential slits into a swirl chamber, giving the liquid a high rotational velocity that, owing to the tangential and axial components of velocity, produces the hollow cone pattern at the circular exit orifice (Matthews, 1992).

A Cartesian coordinate system was used, with *z* in the axial direction. The hollow cone geometry consists of two slits (0.86 mm width, 0.90 mm height) where the fluid enters the nozzle swirl chamber. The upper portion of the swirl chamber consists of a cylinder (2.34 mm radius, 1.03 mm length) that funnels down to another cylinder (0.5435 mm radius, 0.9 mm length), at the end of which is the circular exit orifice. The funnel geometry was created by uniting six frustrums, whose top and bottom radii and heights were determined from the CFE−SEM micrograph by taking incremental measurements of the slope along the funnel surface. To simplify the inflow boundary condition, the nozzle control volume was extended to include the flow that enters in between the outer casing of the nozzle (4.1 mm radius) and the nozzle body itself. There is a core (3.3 mm radius) located above the nozzle swirl chamber so that flow enters the swirl chamber only through the two slits. The grid mesh used in the FLUENT simulations for the TXA8001VK nozzle is presented in figure 5. The volume mesh is a hexahedral and tetrahedral hybrid. The volumes are non−uniform, with the concentration of volumes within the exit orifice region. A total of 190,167 nodes were used in the model, of which 78% of those nodes are located within the funnel and exit orifice region. The grid size within the exit

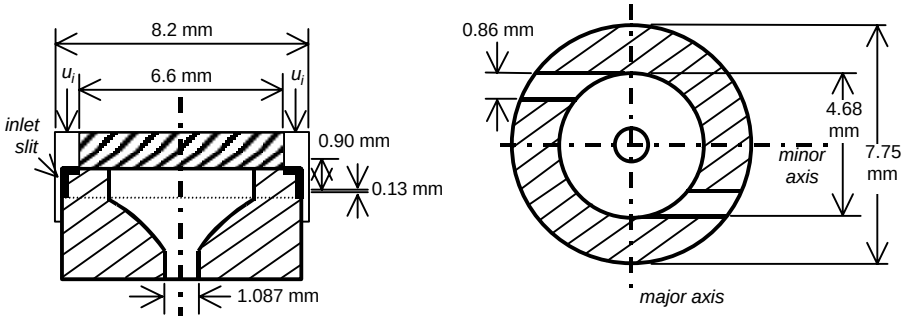

Figure 4. Schematic diagram of the Spraying Systems TXA8001VK hollow cone nozzle.

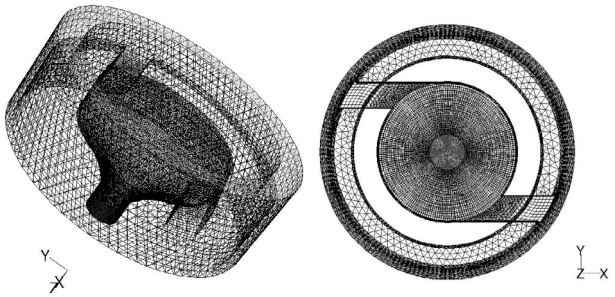

Figure 5. Grid mesh of the TXA8001VK hollow cone nozzle used in FLUENT to simulate the flow field.

orifice region is approximately 20 μm, which is similar in size to the average width of an EPN.

The assumptions for both numerical models were standard (i.e., incompressible fluid, no slip along the walls, fluid is a continuum). In addition, it was assumed that all the experiments were conducted in the laminar regime. The boundary conditions assigned for the models were a uniform velocity profile at the domain inlet and outflow at the domain exit. The fluid medium was water at standard atmospheric conditions. The solver settings (i.e., pressure, pressure−velocity coupling, and under−relaxation) were set to the default.

Simulations of each nozzle's flow field were conducted for each of the experimental flow rates. A user−defined function was created in FLUENT to compute the energy dissipation rate from the flow field information. Several researchers have used energy dissipation rate to characterize local hydrodynamic conditions resulting in cell (Gregoriades et al., 2000; Ma et al., 2002) and organism (Fife et al., 2004) damage because of its practical and theoretical appeal. Mathematically, the energy dissipation rate (eq. 2) captures the local effect of the nine velocity gradients at any given point within a flow field. Practically, the energy dissipation rate represents the rate of viscous energy being dissipated by the fluid element directly to a body that is in the control volume of that fluid element. It is assumed that all the viscous energy being dissipated by the fluid element will be fully realized by the body. The rate of viscous energy dissipated (dQ_f/dt, W) per unit of volume (ΔV, m^3) for three−dimensional flow is computed as follows (Schlichting, 1955):

$$\frac{dQ_f}{dt\Delta V} = \mu\left[2\left(\frac{\partial u_x}{\partial x}^2 + \frac{\partial u_y}{\partial y}^2 + \frac{\partial u_z}{\partial z}^2\right) + \left(\frac{\partial u_y}{\partial x} + \frac{\partial u_x}{\partial y}\right)^2 + \left(\frac{\partial u_z}{\partial y} + \frac{\partial u_y}{\partial z}\right)^2 + \left(\frac{\partial u_z}{\partial x} + \frac{\partial u_x}{\partial z}\right)^2\right] \quad (2)$$

where

μ = fluid viscosity (kg m^{-1} s^{-1})
u_x = x velocity component (m s^{-1})
u_y = y velocity component (m s^{-1})
u_z = z velocity component (m s^{-1}).

The most representative value of the energy dissipation rate within the exit orifice region was determined for each nozzle and for each experimental condition. For the flat fan, the energy dissipation rate values from computational nodes located on cross−sections at 0.0417 mm intervals within the exit orifice tip that forms the elliptical orifice surface were used to compute the average energy dissipation rate. For the hollow cone, the energy dissipation rate values from computational nodes on the circular exit orifice surface were used to compute the average energy dissipation rate. In both cases, the energy dissipation rates from nodes located within 31.75 μm from the nozzle wall were not included in the mean calculation because values near the wall were significantly higher than the bulk flow due to the assumption of no−slip at the wall, and would skew the mean. The distance of 31.75 μm was used in a previous study (Fife et al., 2004) and represents approximately one EPN width from the wall. A MATLAB (Version 6.0, The Mathworks, Inc., Natick, Mass.) program was created to read the energy dissipation values from FLUENT and to compute the average from the values located away from the nozzle wall.

Results and Discussion

Analysis of Nematode Relative Viability

The total pressure changes within the nozzles were estimated from the CFD simulations and were well below the levels cited by Fife et al. (2003) for appreciable EPN damage due to a pressure differential (i.e., 1283 kPa for *H. megidis* and 2183 kPa for *H. bacteriophora* and *S. carpocapsae*).

Table 1 summarizes the observed relative viability of each EPN species with respect to the nozzle and flow treatments.

Table 1. Experimental conditions and observed mean relative viability of *Heterorhabditis bacteriophora, H. megidis, Steinernema carpocapsae*, and *S. glaseri* after treatment with three common types of hydraulic spray nozzles: XR8001VS flat fan (XR), TXA8001VK hollow cone (TXA), and FL5−VS full cone (FL).

Volumetric Flow Rate (L min^{-1})	Entomopathogenic Nematode Relative Viability (%)[a]												
	H. bacteriophora			*H. megidis*			*S. carpocapsae*			*S. glaseri*			
	XR	TXA	FL	XR	TXA	FL	XR	TXA	FL	XR	TXA	FL	Mean
1.3	99.5 aA	99.8 aA	100 aA	97.8 aA	99.1 aA	99.5 aA	99.7 aA	100 aA	100 aA	96.2 aA	99.6 bA	99.4 bA	99.8A
1.7	91.6 aB	99.1 bA	99.6 bA	86.6 aB	98.5 bA	99.6 bA	98.5 aAB	100 bA	100 bA	92.7 aA	91.0 aB	98.8 bA	98.1B
2.1	78.0 aC	91.0 bB	99.7 cA	38.9 aC	93.8 bB	98.7 cA	97.2 aB	99.0 abA	100 bA	47.8 aB	48.5 aC	99.2 bA	89.6C
Mean	89.7a	96.6b	99.8c	74.4a	97.1b	99.3c	98.5a	99.7b	100b	78.9a	79.7a	99.1b	
		95.4a			90.3b			99.4c			85.9d		

[a] Nematode relative viability was quantified by counting the number of living and dead (whole and pieces) EPNs, and the relative viability was computed according to equation 1. Within each EPN species and for the overall mean between EPN species, means in the same row followed by the same lowercase letter do not differ significantly according to the LSD test, $P < 0.05$. Within each nozzle type and for the overall mean between volumetric flow rates, means in the same column followed by the same uppercase letter do not differ significantly according to the LSD test, $P < 0.05$.

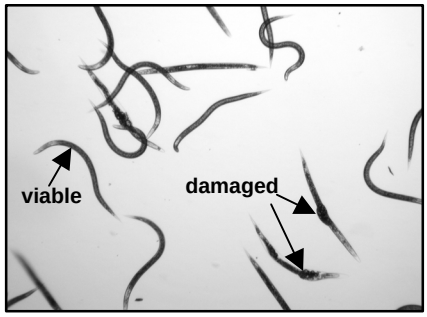

Figure 6. *Heterorhabditis bacteriophora* nematodes (average 588 µm length and 23 µm width) after treatment with the XR8001VS flat fan nozzle at a volumetric flow rate of 2.1 L min^{-1}. When nematodes were damaged due to hydrodynamic stress, Heterorhabditidae nematodes consistently remained whole with an internal rupture (seen above), and Steinernematidae nematodes broke, often into pieces.

From the analysis of variance, differences in mean EPN relative viability among EPN species ($P < 0.001$), among nozzle types ($P < 0.001$), among volumetric flow rates ($P < 0.001$), and for treatment interactions ($P < 0.01$) were all statistically significant. Comparison of individual treatment means provides further insight. Overall, the mean relative viability varied for each EPN species; *S. carpocapsae* experienced little reduction in relative viability (i.e., relative damage) (0.6%, SE = 0.2%), compared to *H. bacteriophora* (4.6%, SE = 1.0%), *H. megidis* (9.7%, SE = 2.6%), and *S. glaseri* (14.1%, SE = 2.9%). An example of damaged *H. bacteriophora* nematodes after flow through the XR8001VS flat fan nozzle is presented in figure 6.

Recent studies have found that *S. carpocapsae* can withstand pressure differentials above 10,000 kPa (Fife et al., 2003) and more intensive hydrodynamic conditions (Fife et al., 2004) compared to the other EPN species. Possible explanations for the observed differences between EPN species were attributed to the ultrastructure properties of the nematode cuticle and size.

The ultrastructure properties of *S. carpocapsae* are known to be more robust than other *Steinernema* spp. (Kondo and Ishibashi, 1989; Patel and Wright, 1998), which supports the minimal damage observed for *S. carpocapsae*. *Heterorhabditis megidis* and *S. glaseri* are considerably larger in size than the other two species, which may have contributed to the higher reductions in relative viability for these two species. To better distinguish the effects of the nematode cuticle and size with respect to EPN damage, more information on structural properties of nematodes from the Heterorhabditidae and Steinernematidae families is needed.

The FL5−VS nozzle exerted no significant reduction in mean EPN relative viability (0.01%, SE = 0.04%) for the range of volumetric flow rates and EPN species tested. The FL5−VS was selected because it is the smallest commercially available nozzle of its type. However, it is considerably larger in size (i.e., larger capacity) compared to the XR8001VS and TXA8001VK nozzles, which are rated similar in flow rates. Direct comparison of the XR8001VS and TXA8001VK nozzles over the range of volumetric flow rates and EPN species shows that the mean relative viability after treatment was significantly lower for the XR8001VS (90.5%, SE = 0.9%) compared to the TXA8001VK (97.2%, SE = 0.6%). In

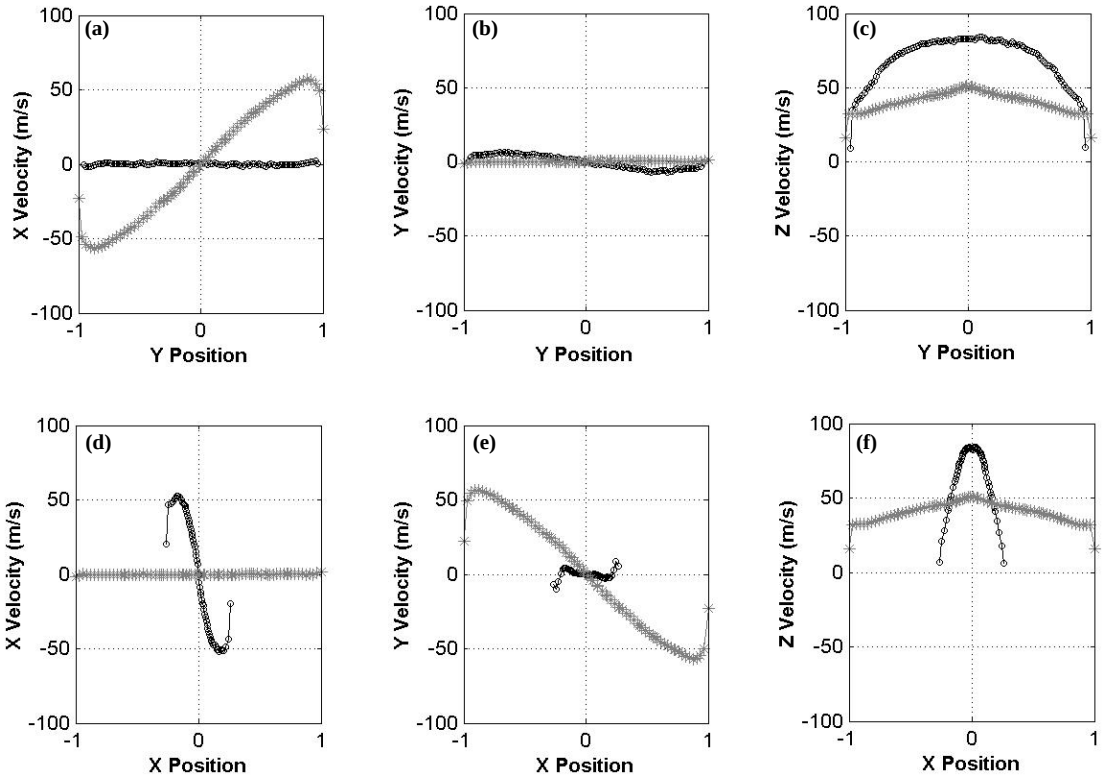

Figure 7. FLUENT simulation results of the *x*, *y*, and *z* velocity (m s^{-1}) components on the (a to c) major and (d to f) minor axes, respectively, of the exit orifices of the XR8001VS flat fan (black circles) and TXA8001VK hollow cone (gray asterisks) nozzles at a volumetric flow rate of 2.1 L min^{-1}. The *y* position (major axis) and *x* position (minor axis) of the plots were normalized by the diameter of the TXA8001VK exit orifice. See figures 2 and 4 for orientation of major and minor axis to orifice for each nozzle.

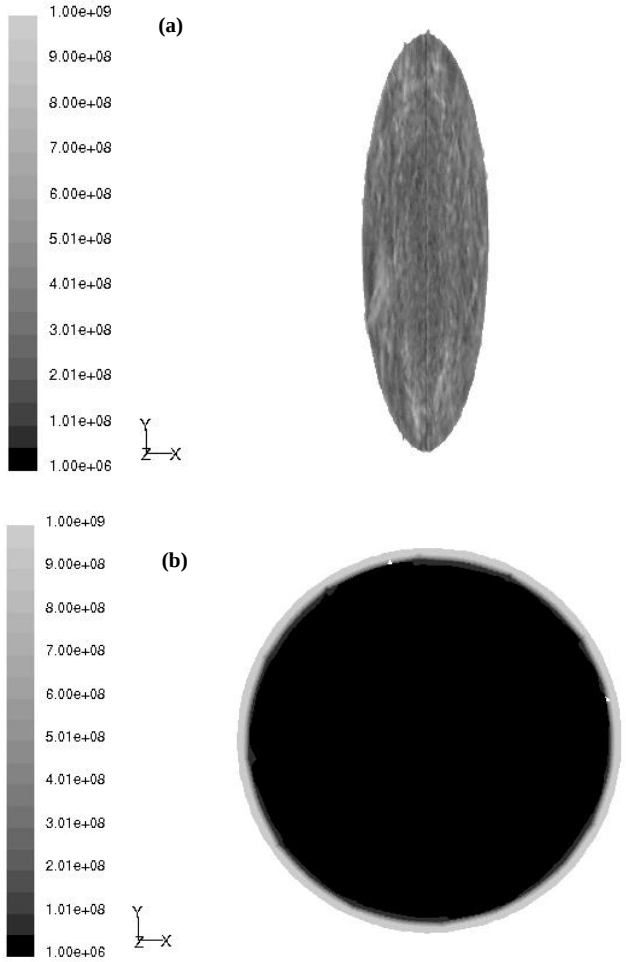

Figure 8. FLUENT simulation results of the energy dissipation rate (W m^{-3}) from the exit orifice surfaces of the (a) XR8001VS flat fan and (b) TXA8001VK hollow cone nozzles at a volumetric flow rate of 2.1 L min^{-1}.

particular, at 2.1 L min^{-1}, the mean relative viability was 13% less for *H. bacteriophora* and 55% less for *H. megidis* after passing through the XR8001VS compared to the TXA8001VK.

Computer Simulation of the Nozzles

The FLUENT simulation results of each nozzle's flow field are consistent with the nozzle characteristics (fig. 7). On the minor axis of the XR8001VS exit orifice, the fluid velocity is primarily composed of an *x* component (fig. 7d) directed toward the center and an axial component (fig. 7f), which would cause the two streams of liquid to meet at the center as described above. On the major axis of the XR8001VS exit orifice, the flow is predominately axial (fig. 7c) since the major axis is aligned with the liquid sheet that forms. For the TXA8001VK nozzle, the tangential (figs. 7a and 7e) and axial (figs. 7c and 7f) components of velocity characterize the rotational flow field that forms the hollow cone at the exit orifice as described above.

Figure 8 presents FLUENT simulation results of the energy dissipation rates on the exit orifice surfaces of the (a) XR8001VS and (b) TXA8001VK nozzles for a volumetric flow rate of 2.1 L min^{-1}. The XR8001VS nozzle has high levels of energy dissipation rate (i.e., >1E+8 W m^{-3}) over the entire elliptical surface, whereas the TXA8001VK nozzle has comparable levels only near the nozzle wall. For each of the three experimental flow conditions (1.3, 1.7, and 2.1 L min^{-1}), the average energy dissipation rates computed in FLUENT within the nozzle exit orifices were 1.1E+8, 1.9E+8, and 2.8E+8 W m^{-3} for the XR8001VS and 5.1E+6, 7.0E+6, and 9.1E+6 W m^{-3} for the TXA8001VK, respectively. Based on results from previous work (Fife et al., 2004), it is recommended that energy dissipation rates within an equipment component should be less than 1E+8 W m^{-3} to avoid hydrodynamic damage to EPNs. For the range of experimental flow conditions, the average energy dissipation rates within the XR8001VS nozzle exceed this threshold, while for the TXA8001VK the values are well below the threshold. The overall greater reductions in EPN relative viability observed after treatment with the XR8001VS compared to the TXA8001VK are consistent with the differences in average energy dissipation rates between the two nozzles.

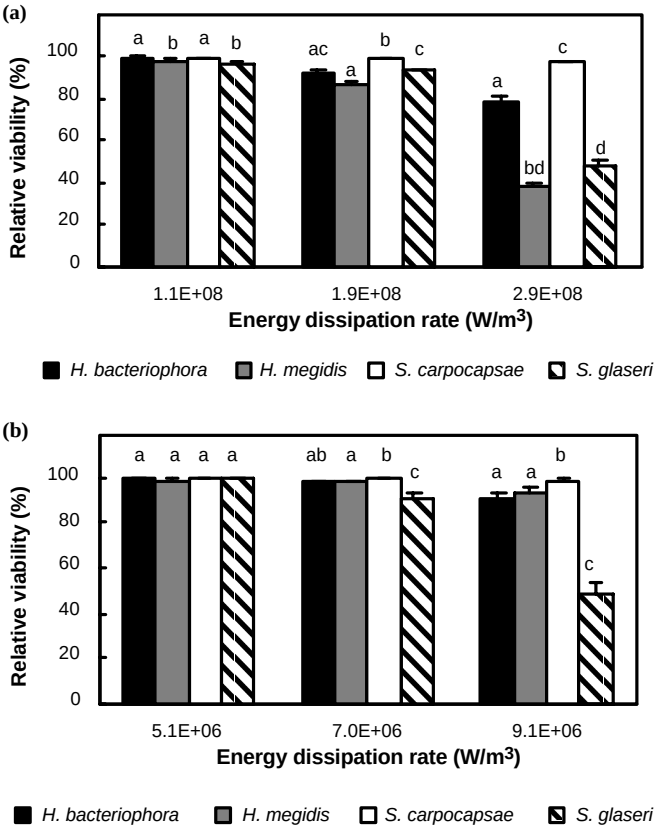

Figure 9. Observed mean relative viability (%) of *Heterorhabditis bacteriophora*, *H. megidis*, *Steinernema carpocapsae*, and *S. glaseri* compared to the average energy dissipation rates (W m^{-3}) computed in FLUENT within the exit orifices of the (a) XR8001VS flat fan and (b) TXA8001VK hollow cone nozzles. Error bars represent standard error of the mean (n = 6).

Figure 9 presents the computed average energy dissipation rates within the (a) XR8001VS and (b) TXA8001VK nozzles compared to the corresponding observed relative viability for *H. bacteriophora*, *H. megidis*, *S. carpocapsae*, and *S. glaseri*. Average energy dissipation rates corresponding to appreciable EPN damage were similar to results reported by Ma et al. (2002), which varied between 7E+7 W m^{-3} and 2E+8 W m^{-3} for damage to animal cells in suspension. However, for the TXA8001VK nozzle, a significant reduction in relative viability of *S. glaseri* (−51.5%, SE = 4.3%) occurred for an average energy dissipation rate of 9.1E+6 W m^{-3}, while appreciable

damage was not observed for the other EPN species at this energy dissipation level. A possible explanation for this anomaly may be the relative size of *S. glaseri* compared to the other EPN species and the nature of the flow within the TXA8001VK nozzle (i.e., swirl). The TXA8001VK exit orifice is similar in size to the length of a *S. glaseri* nematode (i.e., approximately 1 mm). Because of the swirl flow component, the nematodes are unlikely to be aligned lengthwise in the axial direction during flow through the exit orifice. Thus, the relative size of *S. glaseri* may have caused parts of the nematode body to be in close proximity to the nozzle wall, where energy dissipation rates are considerably higher (>1E+8 W m^{-3}) and capable of causing nematode damage.

Comparison of the Flat Fan and Hollow Cone Nozzle Flow Fields

To better understand the differences in energy dissipation rate between the XR8001VS and TXA8001VK flow fields, the nine velocity gradients and corresponding energy dissipation rates obtained from the exit orifice major axis of each nozzle are presented in figures 10 and 11, respectively, for a volumetric flow rate of 2.1 L min^{-1}. The *y* position was normalized by the TXA8001VK exit orifice diameter. For both nozzles, the highest energy dissipation rates occur near the nozzle walls because of the large velocity gradients developed due to the assumption of no−slip at the wall. This is demonstrated by the velocity gradients $\partial u_y / \partial y$ (fig. 10e) and $\partial u_z / \partial y$ (fig. 10f) for the XR8001VS nozzle, and $\partial u_x / \partial y$ (fig. 10d) and $\partial u_z / \partial y$ (fig. 10f) for the TXA8001VK nozzle, where the velocity components on the major axis reduce to zero at the nozzle wall (fig. 7).

Away from the nozzle walls, there is a considerable difference in energy dissipation levels between the XR8001VS and TXA8001VK nozzles (fig. 11). For the XR8001VS nozzle, each of the velocity gradient components contributes to the energy dissipation rate. However, the primary contributions come from the axial flow component described by the velocity gradients $\partial u_z / \partial y$ (fig. 10f), which represents shear flow contributions, and $\partial u_z / \partial z$ (fig. 10i), which represents extensional flow contributions. For the TXA8001VK nozzle, the tangential and axial components of flow contribute to the energy dissipation rate, as seen by the velocity gradients $\partial u_x / \partial y$ (fig. 10d) and $\partial u_y / \partial x$ (fig. 10b), representing the rotational nature of the flow, and $\partial u_z / \partial y$ (fig. 10f), which represents shear flow contributions. Shear flow contributions are present within both nozzles because shear flow is intrinsic to any fluid movement. The difference in energy dissipation levels can be explained by the distinctive flow characteristics of the two nozzles. The energy dissipation rate on the major axis is driven by the extensional flow component (i.e., $\partial u_z / \partial z$) for the XR8001VS nozzle and the rotational flow components (i.e., $\partial u_x / \partial y$ and $\partial u_y / \partial x$) for the TXA8001VK nozzle. The reduced flow area (i.e., contraction) of the narrow, elliptical orifice of the flat fan nozzle causes the fluid to accelerate locally to pass through the orifice. Therefore, considerably larger velocity gradients, and hence energy dissipation rates, are developed

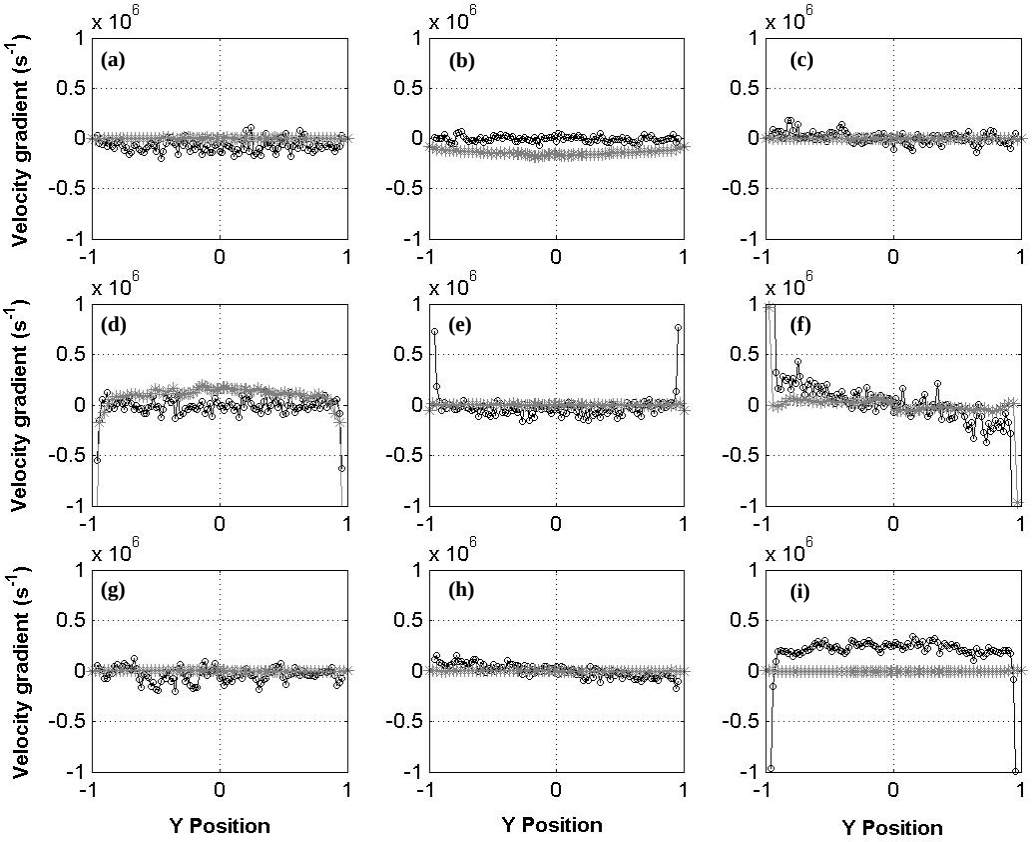

Figure 10. FLUENT simulation results of the velocity gradient (s^{-1}) components on the major axis of the exit orifices of the XR8001VS flat fan (black circles) and TXA8001VK hollow cone (gray asterisks) nozzles at a volumetric flow rate of 2.1 L min^{-1}. The y position was normalized by the diameter of the TXA8001VK exit orifice: (a) $\partial u_x/\partial x$, (b) $\partial u_y/\partial x$, (c) $\partial u_z/\partial x$, (d) $\partial u_x/\partial y$, (e) $\partial u_y/\partial y$, (f) $\partial u_z/\partial y$, (g) $\partial u_x/\partial z$, (h) $\partial u_y/\partial z$, (i) $\partial u_z/\partial z$..

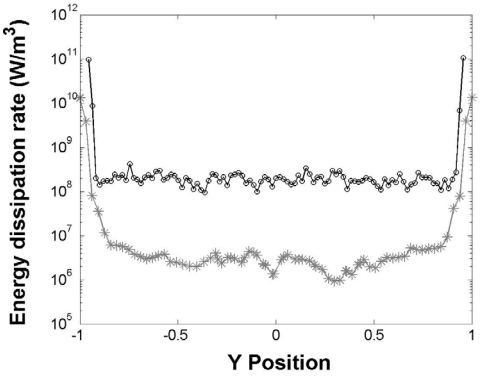

Figure 11. Energy dissipation rates (W m^{-3}) computed in FLUENT on the major axis of the exit orifices of the XR8001VS flat fan (black circles) and TXA8001VK hollow cone (gray asterisks) nozzles at a volumetric flow rate of 2.1 L min^{-1}. The *y* position was normalized by the diameter of the TXA8001VK exit orifice.

within the elliptical orifice tip of the flat fan compared to the circular orifice of the hollow cone.

Several researchers have hypothesized that normal forces arising from an extensional flow are more damaging to a body than purely shear flows at the same level of energy dissipation (Croughan and Wang, 1989; Garcia−Briones and Chalmers, 1994; Gregoriades et al., 2000; McQueen et al., 1987). Fife et al. (2004) provided evidence that supports this hypothesis from an evaluation of the effects of flow through an abrupt contraction on damage to EPNs. Flow into a contraction is characterized by predominately extensional flow at the contraction entrance. The axial velocity gradient (i.e., $\partial u_z / \partial z$), which characterizes an extensional flow, is the defining component for a tensile stress in the axial direction. This previous work found that damaged *Heterorhabditis* nematodes remained whole with an internal rupture and a deformed, necked region located near the center of the nematode body, and damaged *Steinernema* nematodes broke into pieces. The nematode damage can be explained by classic mechanics of materials, where under an ultimate tensile loading (as was experienced during flow into the contraction) a body will exhibit necking at its center and then fail (i.e., break) when the stress becomes too large. In another study (Wilson et al., 2001), an actual tensile load was applied to an adult nematode using calibrated weights hung from a micro−wire attached to one end of the nematode. Similarly, the nematode specimens exhibited necking at the geometric center of the body, and the cuticle appeared to have broken into sections on the uppermost surface. In this case, Wilson et al. (2001) measured the tensile force (5E−2 N) required to cause complete failure of the nematode structural membrane. While in the work of Fife et al. (2004), the tensile forces that were computed in FLUENT during flow into the contraction were considerably smaller (between 1E−4 and 6E−4 N), but large enough to cause deformation that was lethal to the nematodes.

In the current study, after treatment with the XR8001VS nozzle, the nematode damage that was observed (fig. 6) was the same as described above. This indicates that the nematode damage likely resulted from the extensional characteristics of the flow field within the narrow, elliptical orifice of the nozzle. In contrast, the minimal nematode damage observed after treatment with the TXA8001VK nozzle (with the exception of *S. glaseri*, whose relative length may have been a contributing factor) can be attributed to the rotational nature of the flow field at the circular exit orifice of the nozzle, or in other words, a lack of the extensional flow component within the circular exit orifice. Thus, the results from the current study provide further support for the hypothesis that tensile stresses developed within an extensional flow field can be damaging to biological materials.

Nozzle Recommendations

Minimal reductions in EPN relative viability were observed at 1.3 L min^{-1} for the XR8001VS and TXA8001VK, and for the range of experimental conditions for the FL5−VS. Thus, all three of these nozzles are acceptable for spray application of EPNs when following the manufacturer's recommendations. Larger capacity flat fan nozzles (XR8002VS and XR8004VS) were also tested for the same range of experimental conditions, and no significant reductions in EPN relative viability were observed (unpublished data). Larger capacity nozzles are more suitable for EPNs, particularly for soil−applied treatments where a high volume of water is necessary to get the nematodes beyond the soil surface and provide moisture for survival (Grewal and Georgis, 1999). In addition, the cone nozzle size needs to be considered with respect to the EPN length, where larger capacity nozzles should be used for longer EPN species (e.g., *H. megidis*, *S. glaseri*).

In practice, it has generally been considered that EPNs can be applied with conventional spray equipment (Georgis, 1990). The general recommendation has been common nozzle−type sprayers with openings larger than 50 μm and operating pressures less than 2000 kPa (Georgis, 1990), but no studies were cited to support these recommendations. Klein and Georgis (1994) reported that no adverse effects were observed for *Steinernema* spp. and *H. bacteriophora* after flow through several nozzle types (Spraying Systems XR8001VS, TK−VS2, and FL5−VS) but did not report any data explicitly. Thus, the results from this study provide research−based guidelines for selection of appropriate hydraulic nozzles that are consistent with previous, common recommendations for spray application of EPNs.

Finally, the results from this study provide insight into the nozzle characteristics that are least detrimental to a biological agent. In general, based on the flow field characteristics and computed energy dissipation rates, it is recommended that a cone nozzle is more suitable for spray application than a fan nozzle to avoid hydrodynamic damage to biological agents. More information on the tensile strength of different biological agents is necessary to provide specific recommendations. In particular, knowing the relationship between energy dissipation rate and the relative sensitivity of different biological agents will allow determination of which equipment components and operating conditions provide the safest environment for delivery of various biopesticides.

Summary

The flow fields of two common agricultural hydraulic nozzle types (flat fan and hollow cone) were numerically simulated using FLUENT for a range of experimental conditions. There were considerable differences in the average energy dissipation rates within the exit orifices of the XR8001VS and TXA8001VK nozzles for the range of experimental conditions. The significantly greater average reduction in EPN relative viability after treatment with the

XR8001VS nozzle (9.5%) compared to the TXA8001VK nozzle (2.8%) was consistent with the higher computed energy dissipation rates for the XR8001VS. Evaluation of the velocity gradient components on the major axis of each nozzle provided insight into the flow field characteristics associated with the observed nematode damage from the experiments. The reduced flow area of the narrow, elliptical exit orifice of the flat fan nozzle generates an extensional flow regime where the tensile stresses developed are large enough to cause nematode damage. In contrast, the high rotational flow component within the cone nozzle did not produce hydrodynamic conditions conducive to causing appreciable EPN damage, with the exception of one species (*S. glaseri*, whose relative length was approximately the same size as the cone orifice, which may have been a contributing factor to the observed damage). The experimental flow rates in this study were considerably higher than those suggested by the manufacturer for the XR8001VS and TXA8001VK nozzles. Thus, these nozzles are acceptable for spray application of EPNs when following the manufacturer's recommendations. However, it is recommended that larger capacity nozzles be used for EPNs. In particular, the cone nozzle size needs to be considered with respect to the EPN length, where larger capacity nozzles should be used for longer EPN species. In general, based on the flow field characteristics and computed energy dissipation rates, it is recommended that a cone nozzle is more suitable for spray application than a fan nozzle to avoid hydrodynamic damage to biological agents.

ACKNOWLEDGEMENTS

The authors express appreciation to the following organizations for supporting this study: the Ohio Agricultural Research and Development Center (OARDC) at The Ohio State University, the USDA−ARS Application Technology Research Unit, and Spraying Systems Co. for supplying the hydraulic nozzles. Special thanks also to Dr. J. Chalmers and Dr. K. Koelling from the Department of Chemical Engineering at The Ohio State University for use of the experimental flow device, to A. Doklovic and D. Troyer for technical assistance in the experimental set−up, and to L. Horst for technical assistance with the CFE−SEM.

REFERENCES

Bateman, R. P. 1999. Delivery systems and protocols for biopesticides. In *Methods in Biotechnology, Vol. 5: Biopesticides: Use and Delivery*, 509−528. F. R. Hall and J. J. Menn, eds. Totowa, N. J.: Humana Press.

Caulder, J. 1999. The North American scenerio. In *Methods in Biotechnology, Vol. 5: Biopesticides: Use and Delivery*, 13−21. F. R. Hall and J. J. Menn, eds. Totowa, N. J.: Humana Press.

Clay, J. D., and K. W. Koelling. 1997. Molecular degradation of concentrated polystyrene solutions in a fast transient extensional flow. *Polymer Eng. Sci.* 37(5): 789−800.

Copping, L. G., and J. J. Menn. 2000. Biopesticides: A review of their action, applications, and efficacy. *Pest Mgmt. Sci.* 56(8): 651−676.

Croughan, M. S., and D. I. Wang. 1989. Growth and death in overagitated microcarrier cell cultures. *Biotech. Bioeng.* 33(6): 731−744.

Fife, J. P., R. C. Derksen, H. E. Ozkan, and P. S. Grewal. 2003. Effects of pressure differentials on the viability and infectivity of entomopathogenic nematodes. *Biol. Control* 27(1): 65−72.

Fife, J. P., R. C. Derksen, H. E. Ozkan, P. S. Grewal, J. J. Chalmers, and C. R. Krause. 2004. Evaluation of a contraction flow field on hydrodynamic damage to entomopathogenic nematodes − a biological pest control agent. *Biotech. Bioeng.* 86(1): 96−107.

Gan−Mor, S., and G. A. Matthews. 2003. Recent developments in sprayers for application of biopesticides − an overview. *Biosystems Eng.* 84(2): 119−125.

Garcia−Briones, M. A., and J. J. Chalmers. 1994. Flow parameters associated with hydrodynamic cell injury. *Biotech. Bioeng.* 44(9): 1089−1098.

Georgis, R. 1990. Formulation and application technology. In *Entomopathogenic Nematodes in Biological Control*, 173−191. R. Gaugler and H. Kaya, eds. Boca Raton, Fla.: CRC Press.

Gregoriades, N., J. D. Clay, N. Ma, K. W. Koelling, and J. J. Chalmers. 2000. Cell damage of microcarrier cultures as a function of local energy dissipation created by a rapid extensional flow. *Biotech. Bioeng.* 69(2): 171−182.

Grewal, P. S., and R. Georgis. 1999. Entomopathogenic nematodes. In *Methods in Biotechnology, Vol. 5: Biopesticides: Use and Delivery*, 271−299. F. R. Hall and J. J. Menn, eds. Totowa, N. J.: Humana Press.

Jacobsen, B. J., and P. A. Backman. 1993. Biological and cultural plant disease controls: Alternatives and supplements to chemicals in IPM systems. *Plant Dis.* 77(3): 311−315.

Kaya, H. K., and S. P. Stock. 1997. Techniques in insect nematology. In *Manual of Techniques in Insect Pathology*, 281−324. L. A. Lacey, ed. London, U.K.: Academic Press.

Klein, M. G., and R. Georgis. 1994. Application techniques for entomopathogenic nematodes. In *Proc. VI International Colloquium on Invertebrate Pathology and Microbial Control*, 483−484. Knoxville, Tenn.: Society for Invertebrate Pathology.

Kondo, E., and N. Ishibashi. 1989. Ultrastructural characteristics of the infective juveniles of *Steinernema* spp. (Rhabditida: Steinernematidae) with reference to their motility and survivial. *Appl. Entomol. Zool.* 24(1): 103−111.

Ma, N., K. W. Koelling, and J. J. Chalmers. 2002. Fabrication and use of a transient contractional flow device to quantify the sensitivity of mammalian and insect cells to hydrodynamic forces. *Biotech. Bioeng.* 80(4): 428−437.

Matthews, G. A. 1992. *Pesticide Application Methods*. 2nd ed. London, U.K.: Longman Scientific and Technical Publications.

McQueen, A., E. Meilhoc, and J. E. Bailey. 1987. Flow effects on the viability and lysis of suspended mammalian cells. *Biotech. Lett.* 9: 831−836.

Menn, J. J., and F. R. Hall. 1999. Biopesticides. In *Methods in Biotechnology, Vol. 5: Biopesticides: Use and Delivery*, 1−10. F. R. Hall and J. J. Menn, eds. Totowa, N. J.: Humana Press.

Nilsson, U., and E. Gripwall. 1999. Influence of application technique on the viability of biological control agents *Verticillium lecanii* and *Steinernema feltiae*. *Crop Prot.* 18(1): 53−59.

Patel, M. N., and D. J. Wright. 1998. The ultrastructure of the cuticle and sheath of infective juveniles of entomopathogenic Steinernematid nematodes. *J. Helmin.* 72(3): 257−266.

Poinar, G. O., Jr. 1990. Taxonomy and biology of Steinernematidae and Heterorhabditidae. In *Entomopathogenic Nematodes in Biological Control*, 23−61. R. Gaugler and H. Kaya, eds. Boca Raton, Fla.: CRC Press.

SAS. 1994. SAS/STAT User's Guide, Version 6. Cary, N.C.: SAS Institute, Inc.

Schlichting, H. 1955. *Boundary Layer Theory.* 2nd ed. New York, N.Y.: Pergamon Press.

Snedecor, G. W., and W. G. Cochran. 1989. *Statistical Methods.* 8th ed. Ames, Iowa: Iowa State University Press.

Steinke, W. E., and D. K. Giles. 1995. Delivery systems for biorational agents. In *Biorational Pest Control Agents − Formulation and Delivery*, 80−94. F. R. Hall and J. W. Barry, eds. ACS Symp. Series 595. Washington, D.C.: American Chemical Society.

Wilson, J. A., J. D. Pearce, and P. A. Shamlou. 2001. Scalable downstream recovery of nematodes used as biopesticides. *Biotech. Bioeng.* 75(6): 733−740.